Journal of Molecular Liquids 258 (2018) 74–84

Contents lists available at ScienceDirect

Journal of Molecular Liquids

journal homepage: www.elsevier.com/locate/molliq

Antiproliferative activities of procainamide and its binding with calf thymus DNA through multi-spectroscopic and computational approaches

Mohd. Sajid Ali [a,*], Mohammad Abul Farah [b], Hamad A. Al-Lohedan [a], Khalid Mashay Al-Anazi [b]

[a] Department of Chemistry, College of Science, King Saud University, P.O. Box-2455, Riyadh 11451, Saudi Arabia
[b] Department of Zoology, College of Science, King Saud University, P.O. Box-2455, Riyadh 11451, Saudi Arabia

ARTICLE INFO

Article history:
Received 3 December 2017
Received in revised form 4 February 2018
Accepted 20 February 2018
Available online 24 February 2018

Keywords:
Procainamide
Calf thymus DNA
Cytotoxicity
Apoptosis
Fluorescence spectroscopy
Molecular docking

ABSTRACT

The interaction between procainamide with ct-DNA was seen through several experimental and theoretical methods. The fluorescence intensity of procainamide decreased on increasing the concentration of ct-DNA and the quenching process was found to be static with approximately 1:1 binding between ct-DNA and procainamide. UV absorption spectroscopy gave an idea about minor groove binding which was further confirmed by the dye displacement method of DAPI/EtBr bounded ct-DNA interaction. Minor groove binding was also evidenced from the collective information obtained from DNA melting, viscosity and CD spectroscopy. Molecular docking simulations presented that procainamide bound in the minor groove (AT rich) region of B-DNA structures. From thermodynamic point of view the binding interaction between procainamide and ct-DNA was spontaneous process with liberation of energy and overall ordering of system. Hydrogen bonding was found to play important role as suggested by the values of thermodynamic parameters. Whereas from molecular docking simulations it was exposed that hydrogen bonding and hydrophobic interactions were crucial in the binding of ct-DNA and procainamide. DFT method was also used to calculate the Frontier molecular orbitals (HOMO and LUMO) of procainamide which were further used to calculate chemical potential (μ), chemical hardness (η) and fraction number of electrons (ΔN) from procainamide to DNA. Procainamide was found to act as electron donor to DNA bases excpet guanine. Finally, elucidation of anticancer activity revealed that procainamide possesses potential cytotoxicity against MCF-7 breast cancer cells and able to induce significant level of apoptosis at concentrations below IC_{50} value.

1. Introduction

Procainamide is a tertiary amine compound and served as a cardiac depressant, particularly as an antiarrhythmic medicine used to treat cardiac arrhythmic taking place in patients with heart problems. It was developed to upsurge the actual refractory period of the atria and ventricles of the heart [1–4]. Procainamide is quickly absorbed in the body after intravenous or oral administration [5]. It is also associated with several side effects such as, anorexia, vomiting, nausea and diarrhea, fever, joint and muscle pain, etc. [6]. Toxicity of procainamide towards the lungs has also been reported in which it causes the pulmonary fibrosis [7].

Though, it was developed as type IA antiarrhythmic drug, several anticancer activities of procainamide have also been observed [8]. Procainamide was found to protect mice against toxic doses of cisplatin and greatly decreased the weight loss brought by cisplatin. Moreover, it prevented the increased plasma urea nitrogen levels caused by administration of cisplatin as well as the tubular degenerative changes [9]. Procainamide also found to enhance the efficacy of cisplatin in P388 leukemic mice changes [9] as well as increase the tamoxifen response in ERα-positive and ERβ-negative breast cancers [10]. Recently, it was found to improve the anticancer activities of cisplatin against in murine P388, human A2780 and A549 cells [11] and the toxicity of liposome-cisplatin combination was also increased in its presence [12].

Procainamide is also an efficient molecule to design the stable radiolabeling substance for heart imaging [13]. Furthermore, due to its specific binding tendency with melanin pigment, the novel radiotracer was designed for *in vivo* imaging of melanoma tumors [14]. The improvement in the anticholitic activity of 5-aminosalicylic acid was observed when it was conjugated with procainamide via an azo bond [15].

The most interesting role of procainamide as anticancer agent is to promote the demethylation of DNA which is a very important hallmark in cancer related research [16]. DNA demethylation is a practice in which inhibitor distresses the activity of DNA methyltransferases. Procainamide induced demethylation and able to reactivation of the tumor

* Corresponding author.
E-mail address: msali@ksu.edu.sa (M.S. Ali).

https://doi.org/10.1016/j.molliq.2018.02.090
0167-7322/

suppressing genes ER, RARβ3, and p16 in cultured cells [17]. Lee et al. found that procainamide unambiguously prevents the hemimethylase activity of DNA methyltransferase 1 (DNMT1), which is believed to be accountable for maintaining DNA methylation patterns during replication though it was not an effective suppressor of the de novo methyltransferases DNMT3a and DNMT3b2 [18]. Secreted Wingless type (Wnt) ligands are found to be participated in tumor developmental processes and oncogenesis. Aberrant promoter methylation of Wnt inhibitory factor-1 (WIF-1) is a fundamental mechanism of epigenetic silencing in human cancers. Procaine and procainamide were found to reactivate WIF-1 in these cancer cells and downregulate the Wnt canonical pathway subsequently can prevent the development of lung cancer [19].

Since applications of procainamide as anticancer agent are of importance in cancer therapy, study on its interaction and binding mechanism with DNA is of particular interests. DNA is a vital genomic component of life that transports maximum of the hereditary information and permits the biological synthesis of proteins and enzymes through the replication and transcription [20]. Interaction of DNA with small molecules or ligands takes place via various modes for instance (i) intercalation of the small molecule inside the DNA base pairs that causes the distortion in the DNA double helix, (ii) electrostatic interaction between negatively charged phosphate backbone of DNA and positive ends of small molecules, ligands or drugs, (iii) groove binding which involves either minor groove binding preferably for small molecules or major groove binding for large molecules such as polypeptides. Groove binding doesn't influence the double helix of DNA too much unlike intercalation as both are correlated to the grooves in DNA double helix, whereas electrostatic binding takes place outside the groove [21,22].

The binding mode of a drug, in general, and an anticancer drug, in particular, with DNA are gaining attention to evaluate the mechanism of action of the drugs [23–25] because DNA is the prime target of several drug molecules for attenuation the transcription and replication. Understanding the binding mechanism of drug and DNA can be helpful to design the new pharmaceutical agents for targeting DNA [26,27]. Therefore, in the present study we have investigated the mode of binding of procainamide to the ct-DNA experimentally, using a bunch of techniques, as well as computationally using molecular docking and DFT calculations. Furthermore, cytotoxic activities of procainamide on human breast cancer (MCF-7) cells have also been performed. The structure of procainamide is given in Scheme 1.

2. Experimental

UV–visible studies as well as DNA melting studies were performed on Perkin-Elmer Lambda 45 Spectrophotometer using quartz cuvettes of 1 cm path length. Fluorescence spectroscopy was executed on Hitachi F-7000 spectrfluorometer and for quenching experiments the excitation wavelength was 290 nm and the excitation and emission slits were fixed at 10 nm with PMT voltage of 400 V. In case of competitive displacement assays using DAPI and EtBr, the excitation wavelengths were kept as 341 nm and 480 nm, respectively. CD spectroscopy was done on Jasco J-815 spectropolarimeter using 2 mm quartz cell. Ostwald viscometer was used to calculate the relative viscosities of ct-DNA and ct-DNA–procainamide complex. The geometries of procainaimde and DNA bases were optimized at DFT/B3LYP/def2SVP/J [28–30] by ORCA

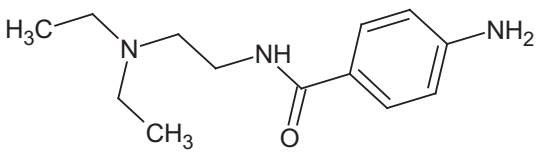

Scheme 1. Structural formula of procainamide.

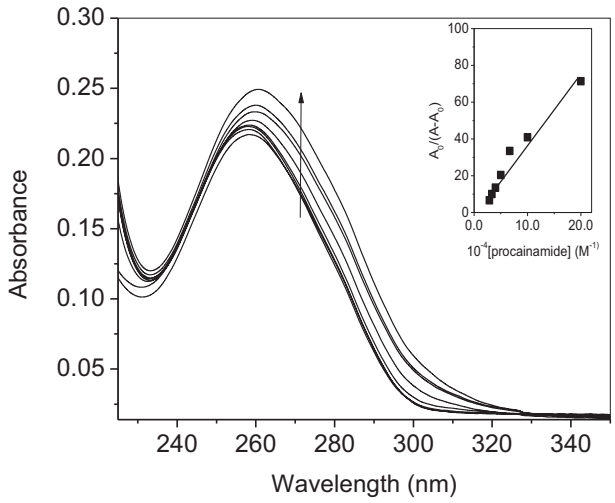

Fig. 1. Difference absorption spectra of ct-DNA (30×10^{-6} M L^{-1}) in presence of increasing amount of procainamide (0, 5, 10, 15, 20, 25, 30, 35×10^{-6} M L^{-1}) at 25 °C. Inset: Benesi Hildebrand plot.

software [31–33]. Autodock 4.2.3 Program was used to perform docking calculations of DNA with procainamide [34].

The MCF-7 human breast adenocarcinoma cell line was obtained from American Type Culture Collection (ATCC, Rockville, MD, USA) and cells were further grown in the lab using standard protocols. A CellTitre 96® non-radioactive cell proliferations assay kit (Promega, Madison, WI, USA) was used to analyze the cytotoxic activity of procainamide through 3-(4,5-dimethylthiazol-2-yl)-2,5-diphenyl tetrazolium bromide (MTT) colorimetric assay. Morphological changes in the cells were observed under a phase contrast inverted microscope equipped with a digital camera (Olympus IX51, Tokyo, Japan) at 100× magnification after growing the cells in presence of various amounts of procainamide. Apoptotic morphological changes were seen by the AO-EtBr dual staining method. The incidence of apoptosis was measured in MCF-7 cells by flow cytometry using the annexin V-FITC and propidium Iodide (PI) apoptosis detection kit (BD Biosciences, San Diego, USA).

The detailed experimental procedure is given in ESI.

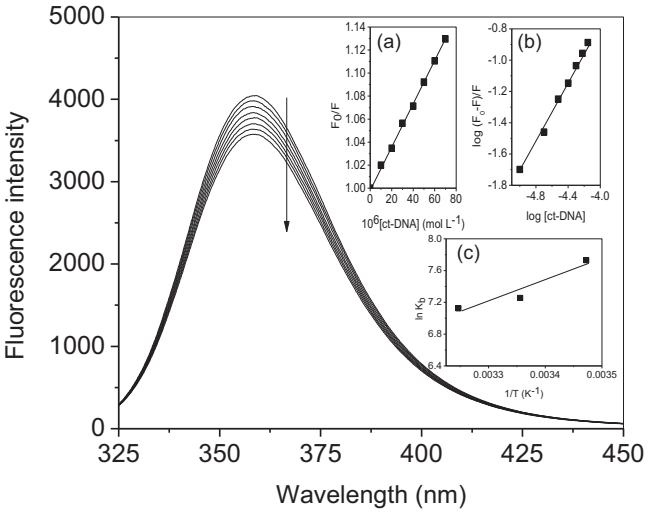

Fig. 2. Fluorescence emission spectra of procainamide (30×10^{-6} M L^{-1}) in the presence of increasing amount of ct-DNA (5, 10, 15, 20, 25, 30×10^{-6} M L^{-1}) at 25 °C. Inset: (a) Stern-Volmer plots of ct-DNA interaction with procainamide. (b) Plot of log $(F_0 - F)/F$ as a function of log [ct-DNA]. (c) van 't Hoff plot of ct-DNA-procainamide interaction.

Table 1
Stern-Volmer quenching constants, binding parameters and thermodynamic parameters for the interaction of ct-DNA with procainamide at various temperatures.

T (K)	Stern-Volmer quenching constants				Binding parameters			Thermodynamic Parameters	
	K_{sv} (M^{-1})		R^2		K_b (M^{-1})	R^2	ΔG (kJ M^{-1})	ΔH (kJ M^{-1})	ΔS (J M^{-1} K^{-1})
288	1.90×10^3	3.33×10^{11}	0.9983	1.04	2.3×10^3	0.9985	−18.4	−22.4	−14.13
298	1.84×10^3	3.22×10^{11}	0.999	0.97	1.4×10^3	0.9968	−18.2		
308	1.80×10^3	3.15×10^{11}	0.9982	0.96	1.2×10^3	0.9962	−18.0		

3. Results and discussions

3.1. Binding of procainamide with ct-DNA using biophysical techniques

3.1.1. UV–visible spectroscopy

UV–visible spectroscopy is imperative technique to understand the binding/interaction between small molecules/ligands and biomacromolecules, for instance proteins and nucleic acids. Procainamide shows specific absorption peak around 290 nm which is the result of the π—π* transitions (Fig. S1) and ct-DNA displays the peak at 260 nm. Fig. 1 is showing the difference UV spectra (the spectra of solutions containing ct-DNA and various amounts of procainamide where the same amount of procainamide was taken as blank) of procainamide–ct-DNA interaction which shows that on the addition of latter the absorbance of former increases, with a small red shift of around 2 nm.

Intercalation of small molecules causes in the red shift followed by the hypochromism due to the coupling of the π-antibonding orbital of small molecules with π-bonding orbital of DNA [27]. Therefore, groove binding is suggested in present case which occurs due to the overlapping of the electronic states of the chromophore of the complex with the nitrogenous bases in the grooves of DNA [35]. Henceforth, from the results obtained using UV–visible spectroscopy it can, primarily, be understood that binding of procainamide is at minor groove of ct-DNA.

The apparent association constant (K_{app}) for the 1:1 procainamide–ct-DNA complex can be calculated according to Benesi-Hildebrand (B-H) equation [27,36]:

$$\frac{A_0}{A_{obs}-A_0} = \frac{\varepsilon_D}{\varepsilon_{P-D}-\varepsilon_D} + \frac{\varepsilon_D}{\varepsilon_{P-D}-\varepsilon_D} \times \frac{1}{K_{app}[procainamide]} \quad (1)$$

where A_{obs} and A_0 are the observed absorbance at 260 nm in presence of procainamide and absorbance of pure ct-DNA, respectively, and ε_D and ε_{P-D} are the absorption coefficients of the ct-DNA and the ct-DNA–procainamide complex, respectively. K_{app} can be determined from the ratio of intercept to slope. From the plots (insets of Fig. 1) the values of K_{app} was found to be 1.8×10^3 M^{-1} which is a suggestive of the minor groove binding as the classical intercalators have a very strong binding and very high binding constants [27]. The value of association constant is in excellent agreement with values of binding constants obtained from the fluorescence quenching measurements and given in the next section.

3.1.2. Fluorescence quenching

Excitation of procainamide at 290 nm yields a fluorescence emission spectrum with a wavelength of emission maximum at 360 nm. This property of procainamide could be used to study the fluorescence quenching with ct-DNA addition. Accordingly, we have studied the effect of [ct-DNA] on the fluorescence quenching of procainamide and the results are given in Fig. 3 as well as Fig. S2 and S3. As the ct-DNA is added to the procainamide solution the fluorescence of the latter is quenches though there was no change in the position of emission maximum. For getting insight on the mechanism of quenching (static or dynamic) we have studied the effect of temperature (Fig. S2 and S3) on the quenching of procainamide by ct-DNA and the quenching mechanism was quantified by the Stern-Volmer equation:

$$\frac{F_0}{F} = 1 + K_{SV}[Q] \quad (2)$$

where F_0 and F are fluorescence intensities in absence and presence of quencher (ct-DNA), respectively, and K_{SV} is Stern-Volmer constant and [Q] is the concentration of quencher.

$$Ksv = k_q \tau_0 \quad (3)$$

where k_q is the bimolecular rate constant of the quenching reaction and $\tau_\circ$ the average integral fluorescence life time of Trp which is ~ 5.7×10^{-9} s [37].

Since in static quenching formation of ground state complex takes place, thus, it is inversely proportional to the temperature whereas in case of dynamic quenching collision between the fluorophore and the quencher takes place and it depends on the molecular diffusion which is increases on increasing the temperature [37,38]. Therefore, studying the system under various conditions of temperature could lead us to determine whether the quenching is static or dynamic. The values of Stern-Volmer constant at various temperatures have been calculated

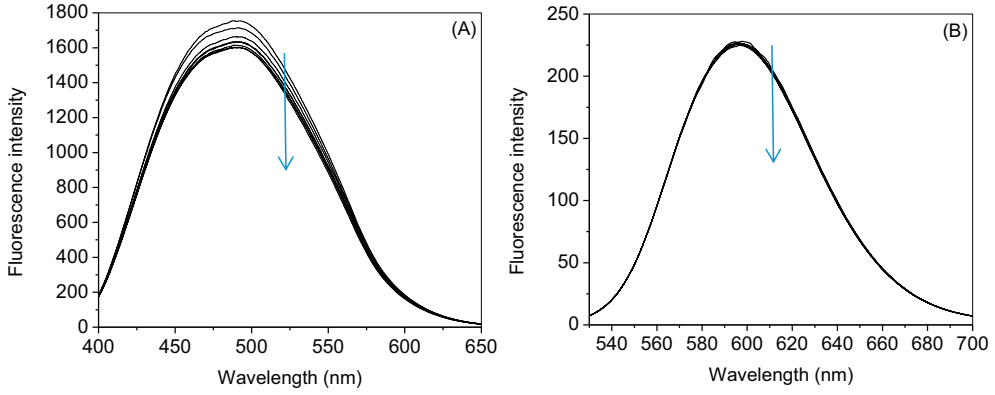

Fig. 3. Competitive displacement assays between procainamide and EtBr/DAPI (A) Fluorescence titration of CT-DNA and DAPI (groove binder) complex with procainamide. DAPI–DNA complex was excited at 338 nm and emission spectra were recorded from 400 to 650 nm. (B) Fluorescence titration of EtBr and CT-DNA with procainamide. EtBr-DNA complex was excited at 471 nm and emission spectra were recorded from 540 to 680 nm. Concentration of procainamide ranges from 0 to 70.0×10^{-6} mol dm^{-3}.

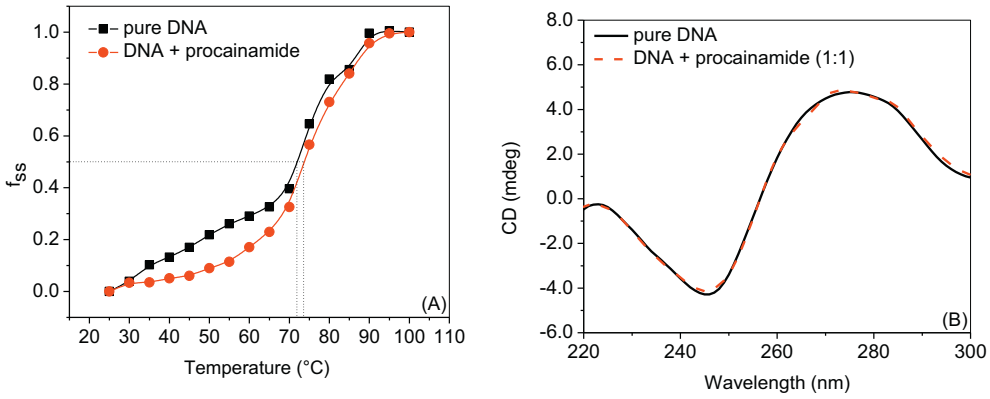

Fig. 4. (A) Melting curves of ct-DNA in the absence and presence of procainamide at pH 7.4. (B) CD spectra of ct-DNA in absence and presence of complex. [procainamide] = 30×10^{-6} mol L^{-1}, and [ct-DNA] = 30×10^{-6} mol L^{-1}.

using linear regression of Eq. 2 and insets A of Fig. 2, Figs. S2 and S3, and the values are of the order of 10^3 this is in support of possibility of groove binding because in case of intercalation K_{SV} are relatively high [39,40]. The inverse dependence of K_{SV} on the temperature (Table 1) clearly establishes the involvement of the static type of mechanism. Further, to support these observations and results the value of the bimolecular rate constant (k_q) was calculated and compared with the limiting diffusion rate constant of the biomolecules (2.0×10^{10} M^{-1} s^{-1}) and the value of k_q was found to be much greater as compared to the latter which again accomplishes that the involvement of static quenching mechanism [41].

3.1.3. Evaluation of binding and thermodynamic parameters

The binding constant (K_b) as well as number of binding sites (n) can be evaluated with the help of the following equation:

$$\log\left(\frac{F_o - F}{F}\right) = \log K_b + n \log [Q] \quad (4)$$

Plots of $\log(F_0-F)/F$ versus log[Q] (Inset (B) of Fig. 2, Figs. S2 and S3) were used to evaluate the binding constants and number of binding sites at various temperatures which are given in Table 1. The K_b obtained at 25 °C is in very close agreement from the one obtained using absorption spectroscopy. From the values of Hill's coefficient, n, it was found that there is 1:1 binding between procainamide and ct-DNA. Once again the values of analyzed binding constants are very less than observed for intercalating molecules, therefore, procainamide can be considered as groove binder [40].

When biomolecules interact with small ligands or molecules, several forces involved in the interactions such as, hydrophobic, van der Waals, electrostatic and hydrogen bonding, can be understood by assessing thermodynamic parameters. There parameters are change in enthalpy (ΔH) and entropy (ΔS) of interaction process along with free energy change (ΔG). The natural logarithm of binding constant is related to the inverse of absolute temperature and can be given as van't Hoff equation (Eq. 4):

$$\ln K = \frac{-\Delta H}{RT} + \frac{\Delta S}{R} \quad (5)$$

From the plots of $\ln K_b$ versus 1/T the values of ΔH *and* ΔS can be calculated which further help to calculate the values of ΔG*:*

$$\Delta G = \Delta H - T\Delta S \quad (6)$$

van't Hoff plot for procaianamide–ct-DNA interaction is given in inset (c) of Fig. 2 and the thermodynamic parameters are enlisted in Table 1. From the negative values of ΔG the feasibility of interaction can be understood. From the values of ΔH and ΔS it can be advocated that the main forces in the interaction between procainamide and ct-DNA are hydrogen bonding and van der walls forces [42]. Theoretical results obtained through molecular docking methods also suggested the involvement of hydrogen bonding.

3.1.4. Competitive binding by dye displacement method

There are several modes of binding by which small molecules binds to the DNA which primarily include the non-covalent and electrostatic interaction and the former is subdivided into intercalation, groove binding (includes major and minor grooves) and external binding [27]. The groove binding mode or intercalation can be identified by the dye displacement assays by using the dyes which are specific to the minor grooves or intercalation sites. For instance, DAPI which binds in the A–T rich regions of double-stranded DNA is a well-known minor groove binder and show a large band in the fluorescence spectrum when bounded to the DNA [43]. If any substance which is a minor groove binder will be added to the DAPI-DNA solution it will compete for the binding site and as a consequence the intensity of DAPI will be decreased. In a similar way EtBr is an intercalator and any intercalating molecule will compete with this molecule for the site if it is bounded to DNA [44].

The effect of procainamide on the DAPI–ct-DNA and EtBr–ct-DNA complex was studied using fluorescence spectroscopy. The results corresponding to DAPI and EtBr have been given in Fig. 3(a) and (b), respectively. Successive addition of procainamide decreases the fluorescence intensity of DAPI whereas the intensity of EtBr remains

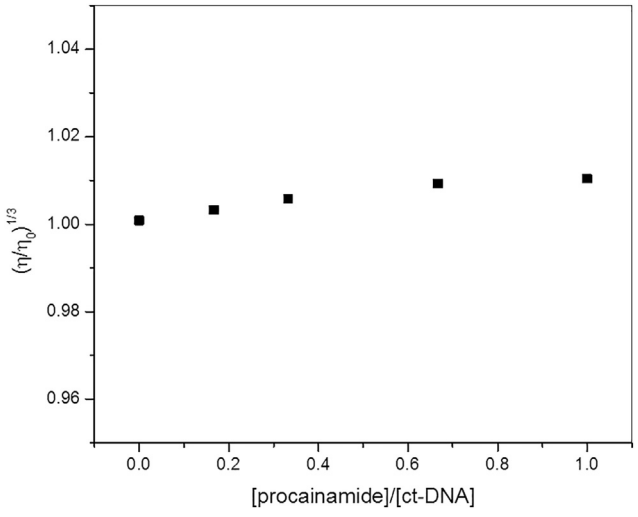

Fig. 5. Effect of increasing amounts of procainamide on the specific viscosity of ct-DNA at pH 7.4. [ct-DNA] = 30×10^{-6} mol L^{-1}.

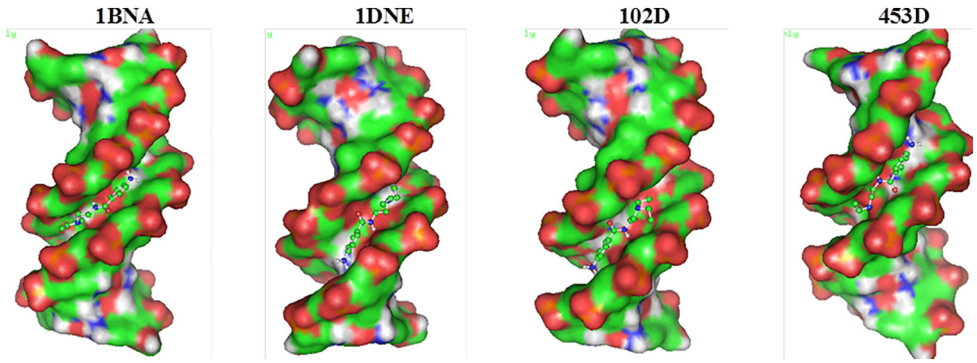

Fig. 6. Molecular docking results of procainamide bound to B-form DNAs.

unchanged. These results clearly indicate that primary site of procainamide binding is on or near minor groove [45].

3.1.5. DNA melting studies

The stability of DNA double helix declines on increasing the temperature due to the weakening of various binding forces. Melting temperature (T_m) is regarded as the temperature at which half of the DNA is melted. In presence of intercalating molecule there is an expected increase of 5–8 °C in the melting temperature of DNA [46] while minor groove binders didn't influence it too much [47]. The T_m of pure ct-DNA and procainamide–ct-DNA complex were achieved from the transition midpoint of the melting curves based on f_{ss} versus temperature (T) according to the following equation [48]:

$$f_{ss} = (A - A_0)/(A_f - A_0) \quad (7)$$

where A_0 and A_f are the initial and final absorbance intensities at 260 nm, respectively, A is the absorbance intensity corresponding to

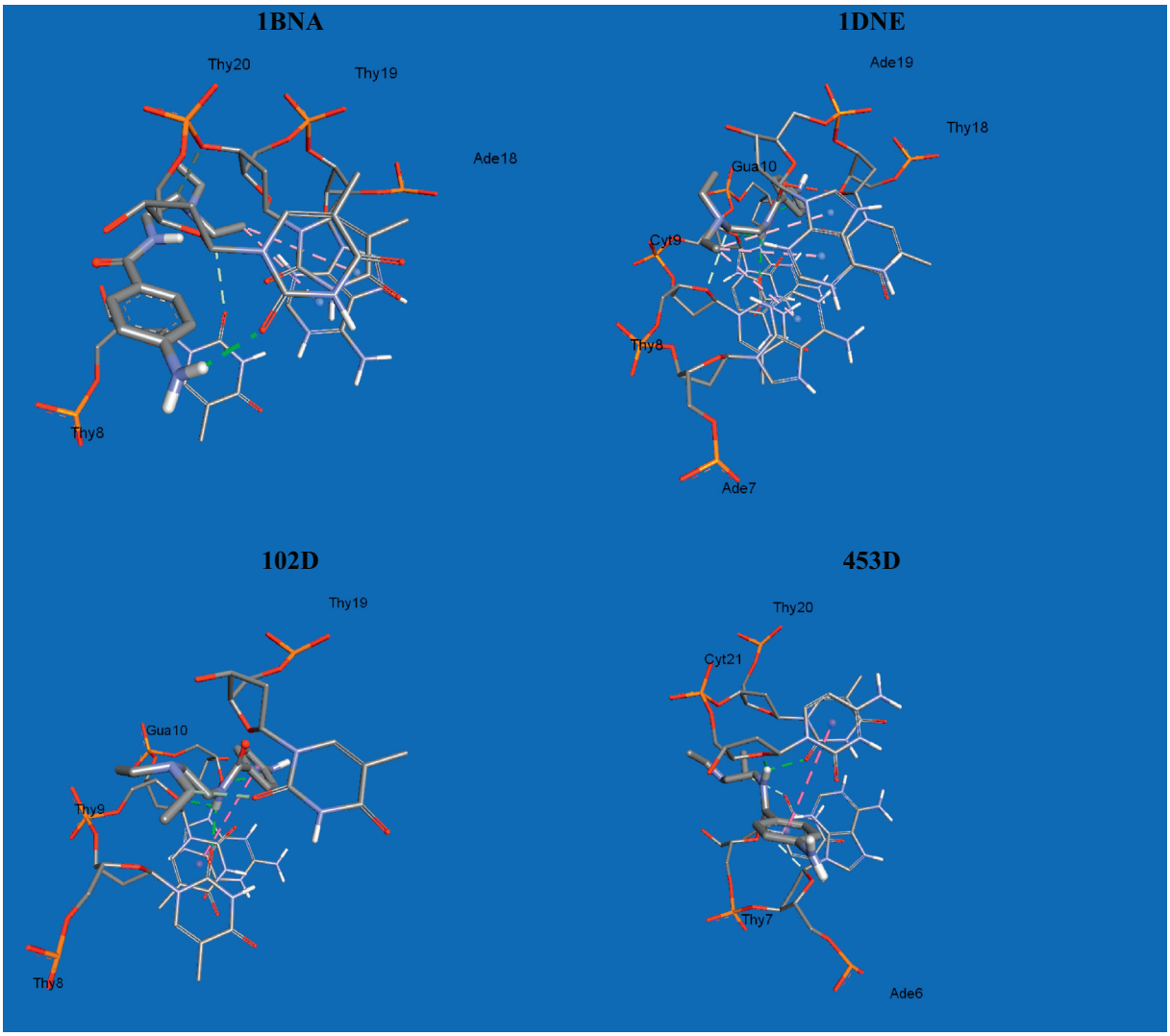

Fig. 7. Predicted binding mode of procainamide docked into DNA.

its temperature and f_{ss} is the fraction of single stranded DNA [49]. The T_m of ct-DNA increases from 72.4 ± 0.2 to 74 ± 0.3 °C in presence of procainamide (Fig. 4(A)) expressive of minor groove binding.

3.1.6. Circular dichroism spectrophotometry

CD spectroscopy can also be employed to apprehend the interaction of small molecules to the DNA. A positive peak at 275 nm in the CD spectrum of ct-DNA is because of the stacking of the base pairs and a negative peak at 245 nm is owing to the polynucleotide helicity (Fig. 4B). If a molecule intercalates the increase in the positive band due to its stacking between the base pairs of DNA takes place [50]. Inversely, interaction of groove binders doesn't influence the CD spectrum too much [24]. Since from the Fig. 4(B), it can be seen that addition of procainamide to the ct-DNA didn't causes any significant change in the CD spectrum of latter and which indicate presence of groove binding between ct-DNA and procainamide. The results obtained here are in good consistency with the observed recently for captopril drug which was found to be minor groove binder [33].

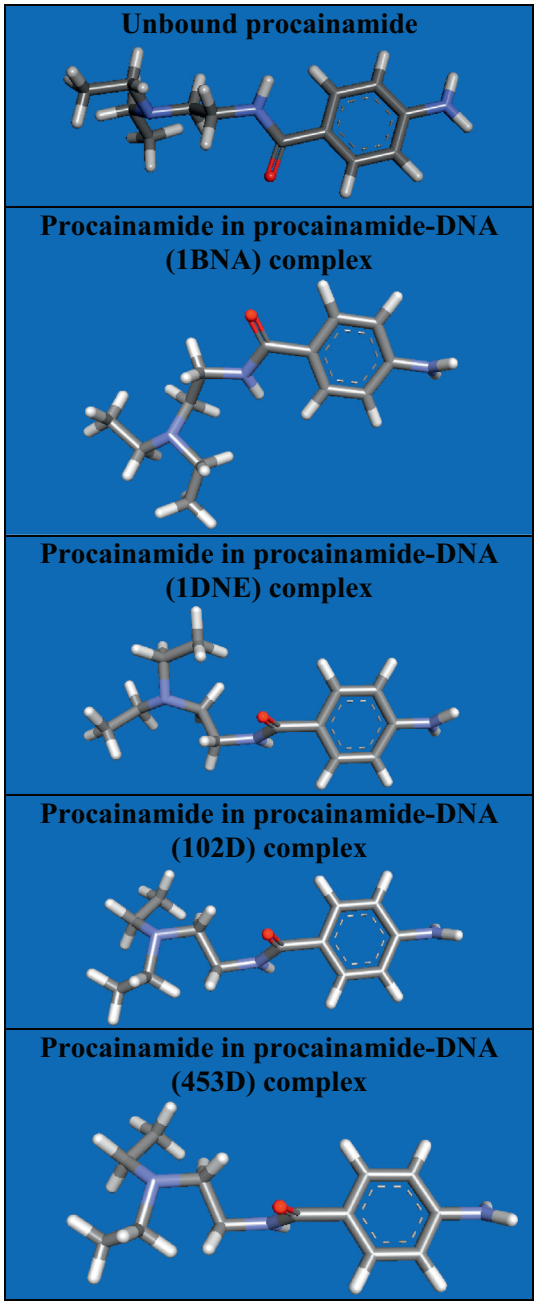

Fig. 8. The conformation of procainamide in procainamide–DNA complexes.

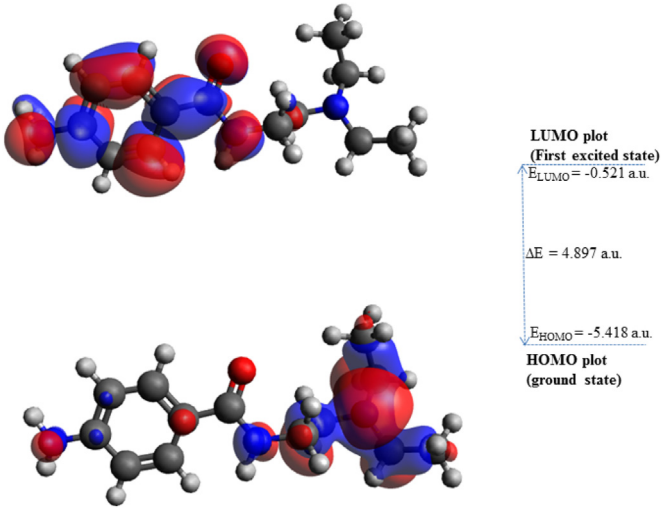

Fig. 9. HOMO–LUMO composition of the frontier molecular orbitals of procainamide.

3.1.7. Viscosity measurements

Viscosity measurements were also performed in order to further verify the site of the interaction (Fig. 5). Viscometry is a classical and easy technique to determine the mode of binding of ligands with DNA. The hydrodynamic changes occurring in the solution can be estimated by use of viscosity measurements. Since an intercalator can enlarge the DNA helix due to the split-up of base pairs at the site consequential in the rise in the relative specific viscosity. On the other hand, the molecules which bind at minor groove didn't split-up the base pairs too much, hence, don't show any noteworthy increase in the viscosity of the DNA. Thus, viscosity measurement can be considered as least elusive method for differentiating between the intercalation and groove binding [51–54]. Effect of various concentrations of procainamide on ct-DNA viscosity was seen and the results are given in Fig. 5. Addition of procainamide causes almost no change in the specific viscosity of ct-DNA, hence, it can further be said that the binding is taking place at minor groove and the similar observations were reported for binding of ct-DNA with some metal complexes and 4,4-dimethylcurcumin [35,45].

3.2. Computational analyses of interaction of procainamide with DNA

3.2.1. Molecular docking

Nowadays use of Computational methods is gaining much interests to design the new chemotherapeutic agents by understanding the specific interactions of small molecules with nucleic acids. Molecular docking has gained too much attention during past decade due to its simple and user friendly approach. It is very convenient to recognize the ligand-biomolecules interactions for the rational drug design and

Table 2
Calculated DFT parameters in a.u. for the procaianmide and DNA bases.

	E_{HOMO}	E_{LUMO}	ΔE	μ	η	ΔN
procainamide	−5.418	−0.521	−4.897	−2.9695	2.4485	
adenine	−6.141	−0.67	−5.471	−3.4055	2.7355	−0.0420
guanine	−5.08	−0.39	−4.69	−2.735	2.345	0.0244
thymine	−5.89	−1.085	−4.805	−3.4875	2.4025	−0.0533
cytosine	−5.917	−0.832	−5.085	−3.3745	2.5425	−0.0405

discovery. The mechanism of the drug-biomolecules interaction can simply be achieved by molecular docking and justification of experimental observations can also be accomplished by these computational approaches [55]. As previously stated, intercalation and groove bindings are the two modes of interaction comes under the domain of non-covalent interactions. The major and minor groove binding also have some difference due to the dissimilar electrostatic potential and steric effects because major groove is somewhat larger than the narrow minor groove which is a suitable site for the small molecules while larger molecules such as polypeptides and polymers have the affinity towards major groove [56].

Molecular docking calculations have been performed on the procainamide-DNA system using four different B-DNA structures from the protein data bank [57] because ct-DNA is a typical B-DNA. The conformer with least binding energy was chosen from the several conformers, given in Fig. 6. It was interesting to note that all the least energy conformers shown the binding at minor groove. The ΔG obtained from the molecular docking method was found to be 21.1 kJ M^{-1} which is more than the one obtained from the experimental methods (Table 1). This ambiguity in the free energy changes obtained through different methods can be explained on the basis that in theoretical calculations we only select the ligand and receptor and the latter is also fixed as rigid entity while in case of wet experiments a number of factors are there such as, presence of solvent and buffer, pH, flexibility of the receptor, etc. which can affect the binding which is not experienced by the molecular docking and, hence, a discrepancy in the values of free energies can be observed [58,59].

The binding pockets for the procainamide in all four B-DNAs are given in Fig. 7. Procainamide binds in the AT rich regions of B-DNA conformers and the mode of binding were hydrogen binding as well as hydrophobic forces (Table S1). The involvement of hydrogen binding in the interaction between procainamide was also analyzed in the experimental results.

Flexibility of procainamide molecule is an important factor in the binding with DNA (Fig. 8). Procainamide molecule adjusts itself accordingly to fix inside the minor groove of DNA.

Earlier, the matching results were reported for the molecular docking studies of an important anticancer drug gafitinib with various types of B-DNA fragments [60]. The drug was found to bind at minor groove in case of all fragments. From the experimental and computational results, it can safely be concluded that the procainamide interacts with ct-DNA through minor groove binding mode and the forces that play important role in the binding are hydrogen bonding, hydrophobic and van der Waals' forces.

3.2.2. DFT calculations

Theoretical prediction of interacting molecules can also be done with the help of molecular modelling using frontier molecular orbitals calculations that include highest occupied molecular orbital (HOMO) and the lowest unoccupied molecular orbital (LUMO) which are important factors for determining the stability of a molecule [28–30,32,33,61].

The geometry of procainamide along with four DNA bases were optimized using ORCA software and HOMO and LUMO were calculated from the optimized structures (Fig. 9 and Fig. S3). The energy associated with HOMO and LUMO were used to calculate the chemical potentials (μ) and chemical hardnesses (η) of system. Which were further used

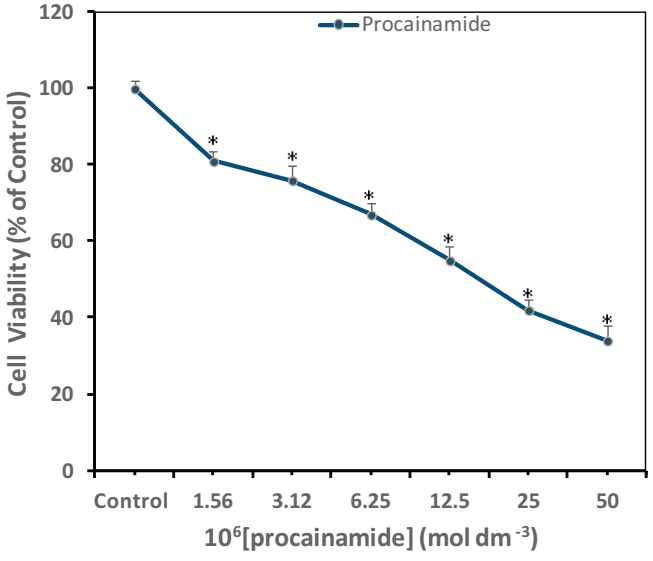

Fig. 10. Cytotoxic effects of procainamide on MCF-7 cells treated as indicated with two-fold dilutions for 24 h. All data are expressed as mean ± SE for three independent experiments. Significant ($p < 0.05$) compared with corresponding controls.

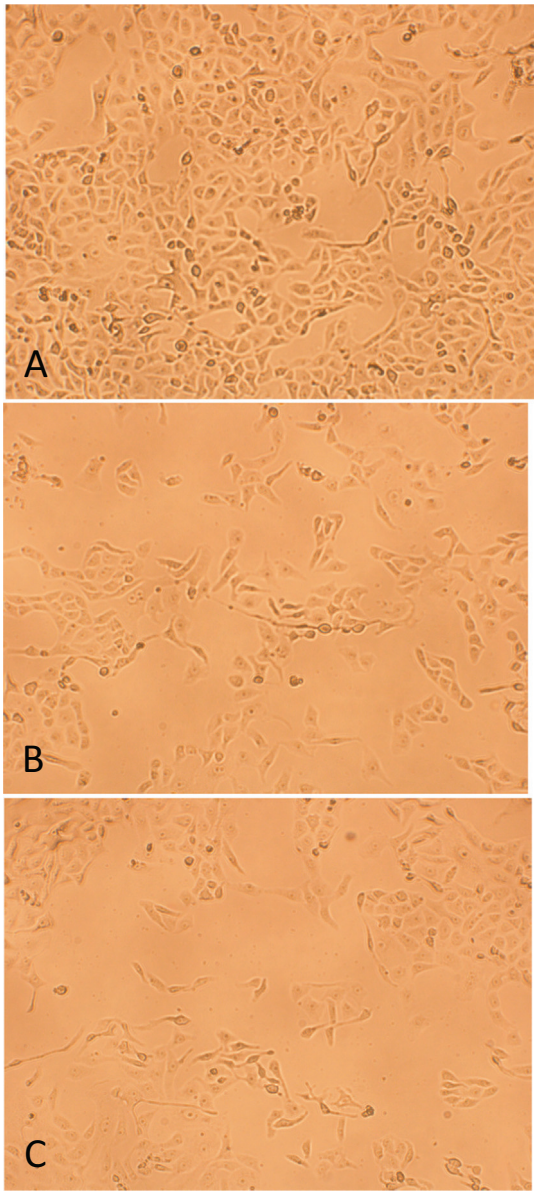

Fig. 11. The MCF-7 cell morphology was examined by phase contrast inverted microscopy. (A) control (B) 5 μM procainamide (C) 10 μM procainamide. Magnification: 100×.

to calculate fraction number of electrons (ΔN) from procainamide to DNA bases.

$$\mu = \frac{E_{LUMO} + E_{HOMO}}{2} \quad (8)$$

$$\eta = \frac{E_{LUMO} - E_{HOMO}}{2} \quad (9)$$

$$\Delta N = \frac{\mu_B - \mu_A}{2(\eta_A + \eta_B)} \quad (10)$$

where μ_A, μ_B and η_A, η_B are the chemical potentials and chemical hardnesses of system A (procainamide) and B (DNA bases), respectively.

The values of η and μ for various substances are given in Table 2. The values of the chemical potential indicate the transfer of electrons from a high chemical potential (less electronegative) system to a low chemical potential (high electronegative) system [62]. It can be stated that procainamide acts as electron donor to the three DNA bases except guanine from which the former accepts electron.

3.3. Antiproliferative and anticancer activities of procainamide

3.3.1. Cytotoxicity of procainamide on MCF-7 cells

Fig. 10 shows the percent viability of cells performed by MTT assay after the MCF-7 cells were exposed to different concentrations of procainamide. A concentration dependent significant ($p < 0.05$) decrease in the cell viability was observed. Cell proliferation was inhibited by 21% at lowest concentration of 1.56 μM and 66% at highest concentration of 50 μM. The IC50 values estimated at 24 h post-treatment in MCF-7 for procainamide is 18 μM. These results suggest that procainamide possesses potential cytotoxicity against MCF-7 cells.

3.3.2. Morphological changes induced by procainamide in MCF-7 cells

The representative image of morphological abnormalities observed under phase contrast inverted microscopy in MCF-7 cells is shown in Fig. 11. MCF-7 cells were treated with 5 and 10 μM of procainamide for 24 h. No significant changes in the morphology were observed in control cells (Fig. 11A). The cells appeared to have a normal shape, were attached to the surface and reached about 95–100% confluence. However, a decreased cell density and some cells round in shape detached from surface was observed in treated MCF-7 cells (Fig. 11B, C).

3.3.3. Apoptotic morphological changes in MCF-7 cells

MCF-7 cells were exposed to procainamide and stained with (AO/EtBr) dye to analyze typical morphological apoptosis changes (Fig. 12). 94.5% of viable cells were observed in control MCF-7 cells. Untreated cells showed evenly distributed AO stain (green fluorescence) with no morphological changes (Fig. 12A). The percentage of viable cells however, decreased significantly ($p < 0.05$) in all treated samples. As shown in Fig. 12B, C, and D, AO/EtBr staining which correlated with the presence of cells with typical apoptotic nuclear morphology (nuclear shrinkage, DNA condensation and fragmentation). Quantification of stained cells revealed that percentage of apoptotic and necrotic cells

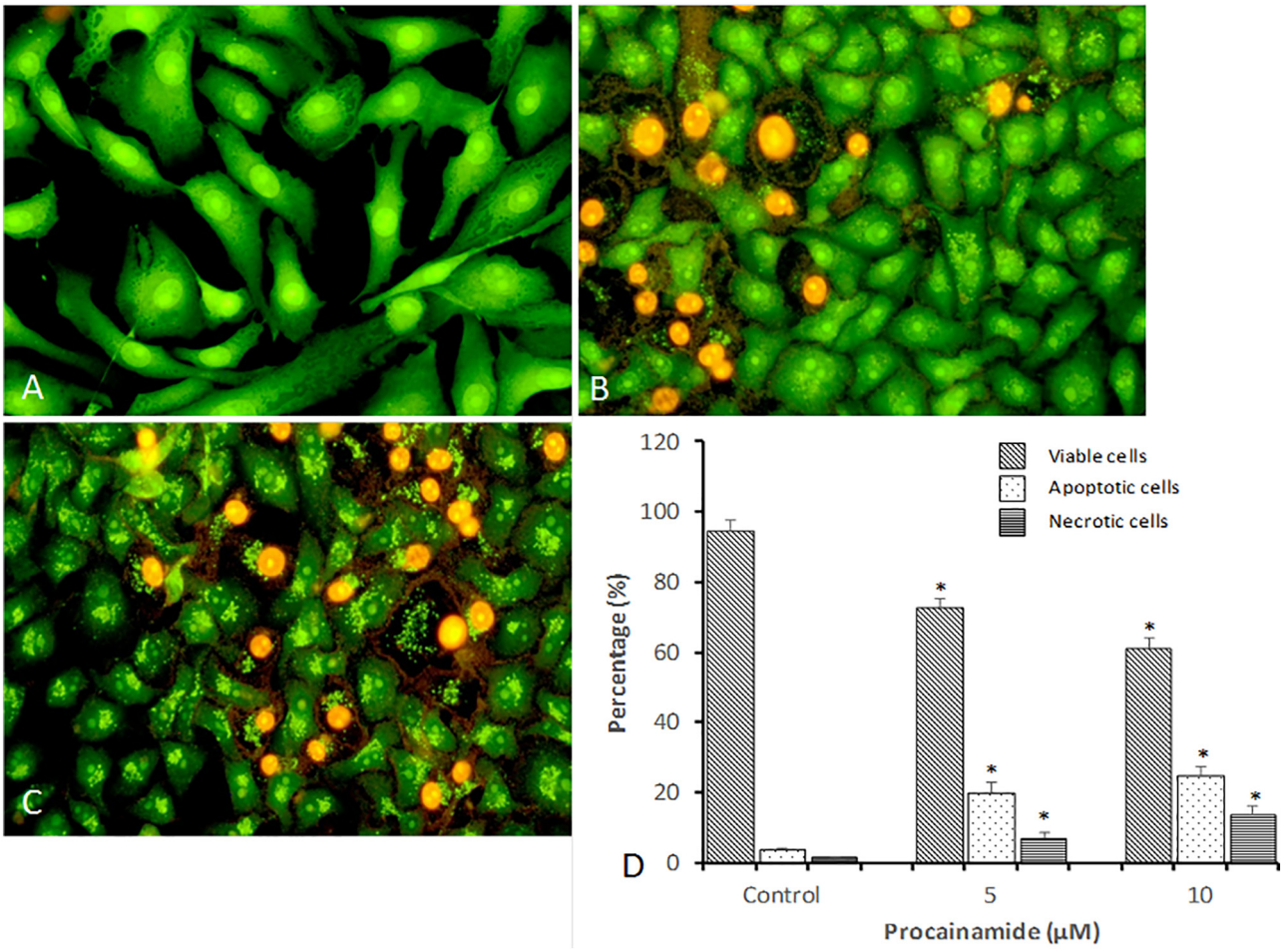

Fig. 12. Typical morphological apoptotic changes in MCF-7 cells observed under fluorescence microscope. (A) Control (B) 5 μM procainamide (C) 10 μM procaiamide. Magnification: 200×. (E) Quantification of normal, apoptotic and necrotic cells based on the staining of AO and EtBr in >300 cells. All data are expressed as mean ± SE for three independent experiments. * Significant ($p < 0.05$) compared with corresponding controls.

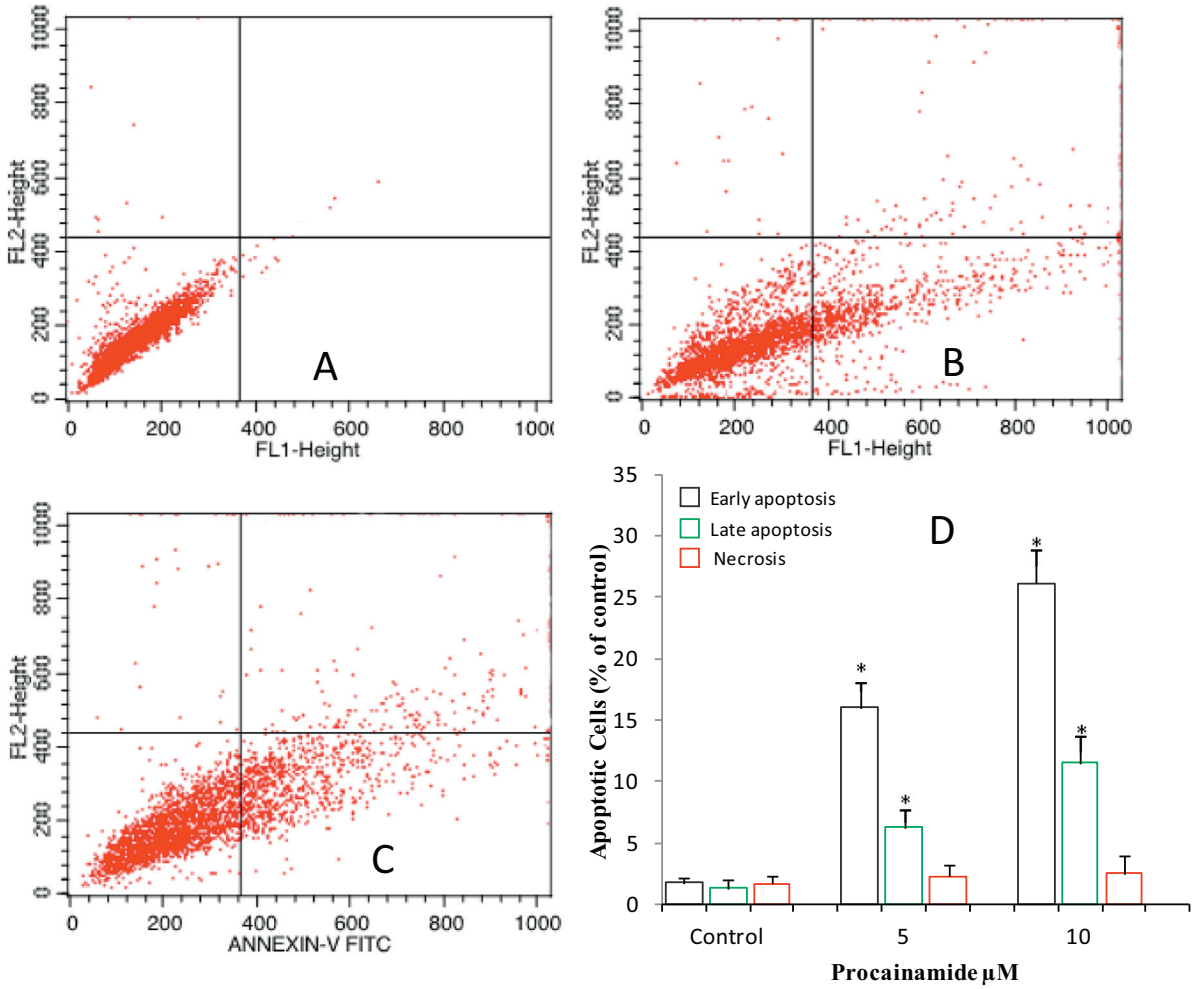

Fig. 13. Dot plots profile of annexin V-FITC/PI assay staining of MCF-7 cells analyzed by flow cytometry showing percentage of viable cells, early apoptosis, late apoptosis and necrotic cells. Cells were exposed to 5 μM procainamide (B) 10 μM procainamide (C) including untreated control (A) for 24 h. (D) Bar diagrams showing the quantitative estimation of early and late apoptosis and necrosis. All data are expressed as mean ± SE. * Significant ($p < 0.05$) compared with corresponding controls independent of three experiments.

increase to 20 ± 3.12 and 7 ± 2.1 respectively, at 5 μM procainamide, while at 10 μM it was 25 ± 2.65 and 14 ± 2.31 respectively (Fig. 12D).

3.3.4. Annexin V-apoptosis assay by flow cytometry

The percentages of early and late apoptotic cells induced by procainamide were determined by double staining with Annexin V and PI via flow cytometry (Fig. 13). Positioning of quadrants on dot plots was designated, and living cells (Annexin V−/PI−), early apoptotic cells (Annexin V+/PI−), late apoptotic cells (Annexin V+/PI+), and necrotic cells (AnnexinV−/PI+) were recognized. These results demonstrate that treatment with procainamide (5 and 10 μM) decreased the population of viable cells and increased the percentage of apoptotic cells. While, in untreated control percentage of apoptotic cells were negligible. As seen in Fig. 13D, percentage of early apoptosis cells increased significantly ($p < 0.05$) to 16 ± 2.1 and 26.1 ± 2.7 in 5 and 10 μM treatment, respectively. Similarly, late apoptotic cells were observed as 6.3 ± 1.5 and 11.5 ± 2.2. In addition, population of necrotic cells was also registered in both the treatments.

The findings of the present study indicate that procainamide is cytotoxic to MCF-7 cells which is attributed to its DNA methylation and DNA minor grove binding characteristics. The latter phenomenon was proved in our molecular docking studies where procainamide was bound in the minor groove (A-T rich) regions of B-DNA structures. Previously, it has been shown that DNA minor grove binding compounds form non-covalent complexes with DNA and cause DNA cleavage in DNA backbones which leads to potent growth inhibition, DNA damage and apoptosis [63]. On the other hand, procainamide causes growth arrest and reactivation of tumor suppressor genes through DNA demethylation in experimental and clinical settings [17,64]. Since procainamide possesses a well characterized safety profile without side effects as an anti-arrhythmic drug, it could be used as anticancer agent that target the DNA molecule to induce cytotoxicity leading to rapidly proliferating cell death.

4. Conclusions

Interaction of ct-DNA with procainamide, an antiarrhythmic drug which is also known to have anticancer properties was seen using experimental and theoretical approaches along with antiproliferative activities of latter towards MCF-7 cells. There was approximately 1:1 binding between ct-DNA and procainamide and the preferred site of binding was minor groove. Both experimental and molecular docking methods were in excellent agreement with each other. The binding between ct-DNA and procainamide was energetically feasible process. The major forces involved in the binding were hydrogen bonding as well as hydrophobic interactions. From DFT method it was established that procainamide acts as electron donor to the DNA bases except for guanine. Interpretation of anticancer activity revealed that procainamide possesses potential cytotoxicity against MCF-7 breast cancer cells and able to induce significant level of apoptosis at concentrations below IC50 value. The overall results also shows that procainamide could be

used as anticancer agent that target the DNA molecule to induce cytotoxicity leading to rapidly proliferating cell death.

Nomenclature
ct-DNA: calf thymus DNA
CD: Circular dichroism
EtBr: Ethidium bromide
DAPI: 4',6-diamidino-2-phenylindole
AO: Acridine orange

Acknowledgement

The authors extend their appreciation to the Deanship of Scientific Research at King Saud University for funding the work through the research group project no. RGP-148.

Appendix A. Supplementary data

Supplementary data to this article can be found online at https://doi.org/10.1016/j.molliq.2018.02.090.

References

[1] C. Ribeiro, A. Longo, Procainamide and Disopyramide, Eur. Heart J. 8 (1987) 11–19.
[2] J.T. Bigger Jr., R.H. Heissenbuttel, The use of procaine amide and lidocaine in the treatment of cardiac arrhythmias, Prog. Cardiovasc. Dis. 11 (1969) 515–534.
[3] J. Kochweser, S.W. Klein, Procainamide dosage schedules, plasma concentrations, and clinical effects, JAMA 215 (1971) 1454.
[4] M.J. Samarin, K.M. Mohrien, C.S. Oliphant, Continuous intravenous antiarrhythmic agents in the intensive care unit: strategies for safe and effective use of amiodarone, lidocaine, and procainamide, Crit. Care Nurs. Q. 38 (2015) 329–344.
[5] J. Kochweser, Pharmacokinetics of procainamide in man, Ann. N. Y. Acad. Sci. 179 (1971) 370.
[6] K. Wang, X. Guan, S. Chai, Q. Zou, X. Zhang, J. Zhang, A novel, molecularly imprinted polymer sensor made using an oligomeric methyl silsesquioxane-TiO2 composite sol on a glassy carbon electrode for the detection of procainamide hydrochloride, Biosens. Bioelectron. 64 (2015) 94–101.
[7] M. Thangam, S. Nathan, M. Petrovica, B. Kar, M. Patel, P. Loyalka, L.M. Buja, I.D. Gregoric, Procainamide-induced pulmonary fibrosis after orthotopic heart transplantation: a case report and literature review, Cardiovasc. Pathol. 24 (2015) 250–253.
[8] A. Duenas-Gonzalez, P. Garcia-Lopez, L.A. Herrera, J.L. Medina-Franco, A. Gonzalez-Fierro, M. Candelaria, The prince and the pauper. A tale of anticancer targeted agents, Mol. Cancer 7 (2008).
[9] M. Esposito, M. Viale, M.O. Vannozzi, A. Zicca, A. Cadoni, F. Merlo, L. Gogioso, Effect of the antiarrhythmic drug procainamide on the toxicity and antitumor activity of cis-diamminedichloroplatinum(II), Toxicol. Appl. Pharmacol. 140 (1996) 370–377.
[10] O. Altundag, K. Altundag, M. Gunduz, DNA methylation inhibitor, procainamide, may decrease the tamoxifen resistance by inducing overexpression of the estrogen receptor beta in breast cancer patients, Med. Hypotheses 63 (2004) 684–687.
[11] M. Viale, C. Fenoglio, D. de Totero, I. Prigione, A. Cassano, A. Vincenti, P. Bocca, R. Gangemi, M.A. Mariggiò, Potentiation of cisplatin-induced antiproliferative and apoptotic activities by the antiarrhythmic drug procainamide hydrochloride, Pharmacol. Rep. 68 (2016) 654–661.
[12] M. Viale, A. Fontana, I. Maric, M. Monticone, G. Angelini, C. Gasbarri, Preparation and Antiproliferative activity of liposomes containing a combination of cisplatin and procainamide hydrochloride, Chem. Res. Toxicol. 29 (2016) 1393–1395.
[13] M.A. Motaleb, I.T. Ibrahim, R.S. Abo Rizq, E.S. Elzanfaly, Preparation, chromatographic evaluation and biodistribution of 99mTc-procainamide as a radiopharmaceutical for heart imaging, Radiochim. Acta (2017) 215.
[14] I. Kertesz, A. Vida, G. Nagy, M. Emri, A. Farkas, A. Kis, J. Angyal, N. Denes, J.P. Szabo, T. Kovacs, P. Bai, G. Trencsenyi, In vivo imaging of experimental melanoma tumors using the novel radiotracer (68)Ga-NODAGA-procainamide (PCA), J. Cancer 8 (2017) 774–785.
[15] W. Kim, J. Nam, S. Lee, S. Jeong, Y. Jung, 5-Aminosalicylic acid azo-linked to procainamide acts as an Anticolitic mutual prodrug via additive inhibition of nuclear factor kappaB, Mol. Pharm. 13 (2016) 2126–2135.
[16] C.-C. Shih, M.-H. Liao, T.-S. Hsiao, H.-P. Hii, C.-H. Shen, S.-J. Chen, S.-M. Ka, Y.-L. Chang, C.-C. Wu, Procainamide inhibits DNA methylation and alleviates multiple organ dysfunction in rats with Endotoxic shock, PLoS One 11 (2016), e0163690.
[17] B. Segura-Pacheco, C. Trejo-Becerril, E. Perez-Cardenas, L. Taja-Chayeb, I. Mariscal, A. Chavez, C. Acuna, A.M. Salazar, M. Lizano, A. Duenas-Gonzalez, Reactivation of tumor suppressor genes by the cardiovascular drugs hydralazine and procainamide and their potential use in cancer therapy, Clin. Cancer Res. 9 (2003) 1596–1603.
[18] B.H. Lee, S. Yegnasubramanian, X.H. Lin, W.G. Nelson, Procainamide is a specific inhibitor of DNA methyltransferase 1, J. Biol. Chem. 280 (2005) 40749–40756.
[19] Z. Gao, Z.D. Xu, M.S. Hung, Y.C. Lin, T. Wang, M. Gong, X.Y. Zhi, D.M. Jablons, L. You, Procaine and procainamide inhibit the Wnt canonical pathway by promoter demethylation of WIF-1 in lung cancer cells, Oncol. Rep. 22 (2009) 1479–1484.
[20] Y. Ni, M. Wei, S. Kokot, Electrochemical and spectroscopic study on the interaction between isoprenaline and DNA using multivariate curve resolution-alternating least squares, Int. J. Biol. Macromol. 49 (2011) 622–628.
[21] R. Bhar, G. Kaur, S.K. Mehta, Exploring interactions of copper hybrid surfactants with calf thymus-DNA, J. Mol. Liq. 241 (2017) 715–721.
[22] A. Haque, I. Khan, S.I. Hassan, M.S. Khan, Interaction studies of cholinium-based ionic liquids with calf thymus DNA: spectrophotometric and computational methods, J. Mol. Liq. 237 (2017) 201–207.
[23] R. Karimi Shervedani, H. Mirhosseini, M. Samiei Foroushani, M. Torabi, F.R. Rahsepar, L. Norouzi-Barough, Immobilization of methotrexate anticancer drug onto the graphene surface and interaction with calf thymus DNA and 4T1 cancer cells, Bioelectrochemistry 119 (2018) 1–9.
[24] S. Afrin, Y. Rahman, T. Sarwar, M.A. Husain, A. Ali, Shamsuzzaman, M. Tabish, Molecular spectroscopic and thermodynamic studies on the interaction of anti-platelet drug ticlopidine with calf thymus DNA, Spectrochim. Acta A Mol. Biomol. Spectrosc. 186 (2017) 66–75.
[25] A. Mukherjee, B. Singh, Binding interaction of pharmaceutical drug captopril with calf thymus DNA: a multispectroscopic and molecular docking study, J. Lumin. 190 (2017) 319–327.
[26] O. Kennard, DNA-drug interactions, Pure Appl. Chem. 65 (1993) 1213–1222.
[27] M. Sirajuddin, S. Ali, A. Badshah, Drug-DNA interactions and their study by UV-visible, fluorescence spectroscopies and cyclic voltametry, J. Photochem. Photobiol. B 124 (2013) 1–19.
[28] S.K. Saha, A. Hens, N.C. Murmu, P. Banerjee, A comparative density functional theory and molecular dynamics simulation studies of the corrosion inhibitory action of two novel N-heterocyclic organic compounds along with a few others over steel surface, J. Mol. Liq. 215 (2016) 486–495.
[29] S.K. Saha, P. Ghosh, A. Hens, N.C. Murmu, P. Banerjee, Density functional theory and molecular dynamics simulation study on corrosion inhibition performance of mild steel by mercapto-quinoline Schiff base corrosion inhibitor, Phys. E. 66 (2015) 332–341.
[30] S.K. Saha, A. Dutta, P. Ghosh, D. Sukul, P. Banerjee, Adsorption and corrosion inhibition effect of Schiff base molecules on the mild steel surface in 1 M HCl medium: a combined experimental and theoretical approach, Phys. Chem. Chem. Phys. 17 (2015) 5679–5690.
[31] F. Neese, Software update: the ORCA program system, version 4.0, Wires Comput. Mol. Sci. 8 (2018).
[32] S.K. Saha, M. Murmu, N.C. Murmu, P. Banerjee, Evaluating electronic structure of quinazolinone and pyrimidinone molecules for its corrosion inhibition effectiveness on target specific mild steel in the acidic medium: a combined DFT and MD simulation study, J. Mol. Liq. 224 ((2016) 629–638.
[33] D. Sukul, A. Pal, S. Mukhopadhyay, S.K. Saha, P. Banerjee, Electrochemical behaviour of uncoated and phosphatidylcholine coated copper in hydrochloric acid medium, J. Mol. Liq. 249 (2018) 930–940.
[34] G.M. Morris, R. Huey, W. Lindstrom, M.F. Sanner, R.K. Belew, D.S. Goodsell, A.J. Olson, AutoDock4 and AutoDockTools4: automated docking with selective receptor flexibility, J. Comput. Chem. 30 (2009) 2785–2791.
[35] C. Metcalfe, C. Rajput, J.A. Thomas, Studies on the interaction of extended terpyridyl and triazine metal complexes with DNA, J. Inorg. Biochem. 100 (2006) 1314–1319.
[36] H.A. Benesi, J.H. Hildebrand, A spectrophotometric investigation of the interaction of iodine with aromatic hydrocarbons, J. Am. Chem. Soc. 71 (1949) 2703–2707.
[37] M.S. Ali, H.A. Al-Lohedan, Deciphering the interaction of procaine with bovine serum albumin and elucidation of binding site: a multi spectroscopic and molecular docking study, J. Mol. Liq. 236 (2017) 232–240.
[38] Quenching of fluorescence, in: J.R. Lakowicz (Ed.), Principles of Fluorescence Spectroscopy, Springer US, Boston, MA 2006, pp. 277–330.
[39] A. Paul, S. Bhattacharya, Chemistry and biology of DNA-binding small molecules, Curr. Sci. 102 (2012) 212–231.
[40] S. Kashanian, J. Ezzati Nazhad Dolatabadi, In vitro studies on calf thymus DNA interaction and 2-tert-butyl-4-methylphenol food additive, Eur. Food Res. Technol. 230 (2010) 821–825.
[41] M.R. Eftink, Fluorescence Quenching Reactions, in: T.G. Dewey (Ed.), Biophysical and Biochemical Aspects of Fluorescence Spectroscopy, Springer US, Boston, MA 1991, pp. 1–41.
[42] S. Naveenraj, S. Anandan, Binding of serum albumins with bioactive substances - nanoparticles to drugs, J. Photochem. Photobiol. C 14 (2013) 53–71.
[43] E.N. Zaitsev, S.C. Kowalczykowski, Binding of double-stranded DNA by Escherichia coli RecA protein monitored by a fluorescent dye displacement assay, Nucleic Acids Res. 26 (1998) 650–654.
[44] S. Mukherjee, I. Mitra, V.P. Reddy B, C. Fouzder, S. Mukherjee, S. Ghosh, U. Chatterji, S.C. Moi, Effect of Pt(II) complexes on cancer and normal cells compared to clinically used anticancer drugs: cell cycle analysis, apoptosis and DNA/BSA binding study, J. Mol. Liq. 247 (2017) 126–140.
[45] B.-M. Liu, C.-L. Bai, J. Zhang, Y. Liu, B.-Y. Dong, Y.-T. Zhang, B. Liu, In vitro study on the interaction of 4,4-dimethylcurcumin with calf thymus DNA, J. Lumin. 166 (2015) 48–53.
[46] S.Y. Bi, H.Q. Zhang, C.Y. Qiao, Y. Sun, C.M. Liu, Studies of interaction of emodin and DNA in the presence of ethidium bromide by spectroscopic method, Spectrochim. Acta A 69 (2008) 123–129.
[47] F.A. Qais, K.M. Abdullah, M.M. Alam, I. Naseem, I. Ahmad, Interaction of capsaicin with calf thymus DNA: a multi-spectroscopic and molecular modelling study, Int. J. Biol. Macromol. 97 (2017) 392–402.
[48] P. Zhao, J.W. Huang, W.J. Mei, J. He, L.N. Ji, DNA binding and photocleavage specificities of a group of tricationic metalloporphyrins, Spectrochim. Acta A 75 (2010) 1108–1114.
[49] X. Zhou, G. Zhang, J. Pan, Groove binding interaction between daphnetin and calf thymus DNA, Int. J. Biol. Macromol. 74 (2015) 185–194.

[50] V. Uma, M. Kanthimathi, T. Weyhermuller, B.U. Nair, Oxidative DNA cleavage mediated by a new copper(II) terpyridine complex: crystal structure and DNA binding studies, J. Inorg. Biochem. 99 (2005) 2299–2307.
[51] L.S. Lerman, Citation classic - structural considerations in the interaction of DNA and Acridines, cc, Life Sci. (1984) 19.
[52] S. Satyanarayana, J.C. Dabrowiak, J.B. Chaires, Neither Delta-Tris(Phenanthroline)ruthenium(ii) nor Lambda-Tris(Phenanthroline)ruthenium(ii) binds to DNA by classical intercalation, Biochemistry 31 (1992) 9319–9324.
[53] J.M. Kelly, A.B. Tossi, D.J. Mcconnell, C. Ohuigin, A study of the interactions of some Polypyridylruthenium(ii) complexes with DNA using fluorescence spectroscopy, Topoisomerization and thermal-denaturation, Nucleic Acids Res. 13 (1985) 6017–6034.
[54] I. Haq, P. Lincoln, D. Suh, B. Norden, B.Z. Chowdhry, J.B. Chaires, Interaction of . DELTA.- and .LAMBDA.-[Ru(phen)2DPPZ]2+ with DNA: a calorimetric and equilibrium binding study, J. Am. Chem. Soc. 117 (1995) 4788–4796.
[55] R. Rohs, I. Bloch, H. Sklenar, Z. Shakked, Molecular flexibility in ab initio drug docking to DNA: binding-site and binding-mode transitions in all-atom Monte Carlo simulations, Nucleic Acids Res. 33 (2005) 7048–7057.
[56] R. Corradini, S. Sforza, T. Tedeschi, R. Marchelli, Chirality as a tool in nucleic acid recognition: principles and relevance in biotechnology and in medicinal chemistry, Chirality 19 (2007) 269–294.
[57] H.M. Berman, J. Westbrook, Z. Feng, G. Gilliland, T.N. Bhat, H. Weissig, I.N. Shindyalov, P.E. Bourne, The Protein Data Bank, Nucleic Acids Res. 28 (2000) 235–242.
[58] K. Atkovska, S.A. Samsonov, M. Paszkowski-Rogacz, M.T. Pisabarro, Multipose binding in molecular docking, Int. J. Mol. Sci. 15 (2014) 2622–2645.
[59] H.S. Lee, S. Jo, H.-S. Lim, W. Im, Application of binding free energy calculations to prediction of binding modes and affinities of MDM2 and MDMX inhibitors, J. Chem. Inf. Model. 52 (2012) 1821–1832.
[60] J.-H. Shi, T.-T. Liu, M. Jiang, J. Chen, Q. Wang, Characterization of interaction of calf thymus DNA with gefitinib: spectroscopic methods and molecular docking, J. Photochem. Photobiol. B Biol. 147 (2015) 47–55.
[61] J. Padmanabhan, R. Parthasarathi, V. Subramanian, P.K. Chattaraj, Group philicity and electrophilicity as possible descriptors for modeling ecotoxicity applied to chlorophenols, Chem. Res. Toxicol. 19 (2006) 356–364.
[62] Y.Q. Wang, H.M. Zhang, Exploration of binding of bisphenol A and its analogues with calf thymus DNA by optical spectroscopic and molecular docking methods, J. Photochem. Photobiol. B 149 (2015) 9–20.
[63] X.B. Zhang, S.C. Zhang, D.J. Sun, J. Hu, A. Wali, H. Pass, F. Fernandez-Madrid, M.R. Harbut, N.M. Tang, New insight into the molecular mechanisms of the biological effects of DNA minor groove binders, PLoS One 6 (2011).
[64] Y.S. Lin, A.Y. Shaw, S.G. Wang, C.C. Hsu, I.W. Teng, M.J. Tseng, T.H.M. Huang, C.S. Chen, Y.W. Leu, S.H. Hsiao, Identification of novel DNA methylation inhibitors via a two-component reporter gene system, J. Biomed. Sci. 18 (2011).